Inorganic Chemistry

Communication

pubs.acs.org/IC

High-Pressure Synthesis, Crystal Structure, and Unusual Valence State of Novel Perovskite Oxide $CaCu_3Rh_4O_{12}$

Ikuya Yamada,*[,†,‡,§] Mikiko Ochi,[‡] Masaichiro Mizumaki,[∥,⊥] Atsushi Hariki,[#] Takayuki Uozumi,[#] Ryoji Takahashi,[‡] and Tetsuo Irifune[¶]

[†]Nanoscience and Nanotechnology Research Center, Osaka Prefecture University, 1-2 Gakuen-cho, Naka-ku, Sakai, Osaka 599-8570, Japan

[‡]Department of Chemistry, Graduate School of Science and Engineering and [¶]Geodynamics Research Center, Ehime University, 2-5 Bunkyo-cho, Matsuyama, Ehime 790-8577, Japan

[§]Precursory Research for Embryonic Science and Technology, Japan Science and Technology Agency, 4-1-8 Honcho, Kawaguchi, Saitama 332-0012, Japan,

[∥]Japan Synchrotron Radiation Research Institute, Sayo-cho, Sayo-gun, Hyogo 679-5198, Japan

[⊥]Core Research for Evolutional Science and Technology, Japan Science and Technology Agency, 5 Sanbancho, Chiyoda-ku, Tokyo 102-0075, Japan

[#]Department of Mathematical Sciences, Graduate School of Engineering, Osaka Prefecture University, 1-1 Gakuen-cho, Naka-ku, Sakai, Osaka 599-8570, Japan

Supporting Information

ABSTRACT: A novel perovskite oxide, $CaCu_3Rh_4O_{12}$, has been synthesized under high-pressure and high-temperature conditions (15 GPa and 1273 K). Rietveld refinement of synchrotron X-ray powder diffraction data indicates that this compound crystallizes in a cubic $AA'_3B_4O_{12}$-type perovskite structure. Synchrotron X-ray absorption and photoemission spectroscopy measurements reveal that the Cu and Rh valences are nearly trivalent. The spectroscopic analysis based on calculations suggests that the appropriate ionic model of this compound is $Ca^{2+}Cu^{\sim 2.8+}{}_3Rh^{\sim 3.4+}{}_4O_{12}$, as opposed to the conventional $Ca^{2+}Cu^{2+}{}_3Rh^{4+}{}_4O_{12}$. The uncommon valence state of this compound is attributed to the relative energy levels of the Cu 3d and Rh 4d orbitals, in which the large crystal-field splitting energy of the Rh 4d orbitals is substantial.

Transition-metal (TM) oxides have been extensively studied during the past several decades because of their various electronic properties such as metal−insulator transitions, magnetotransport, and superconductivity.[1] Perovskite oxides, ABO_3, and their derivatives have been widely investigated because of the facile adjustability of their crystal structures and electronic states, which result in intriguing functions and properties. Recently, quadruple A-site-ordered perovskite oxides, $AA'_3B_4O_{12}$ (see the crystal structure in the inset of Figure 1, drawn using *VESTA* software[2]), have been extensively investigated because of the diverse interactions between constituent TM ions at pseudo-square-planar-coordinated A′ sites and octahedrally coordinated B sites, which lead to remarkable features such as a giant dielectric constant in $CaCu_3Ti_4O_{12}$,[3] a colossal magnetoresistance in $LaCu_3Mn_4O_{12}$,[4] and a large negative thermal expansion in $SrCu_3Fe_4O_{12}$.[5] Valence states of $AA'_3B_4O_{12}$-type compounds are not simply determined because

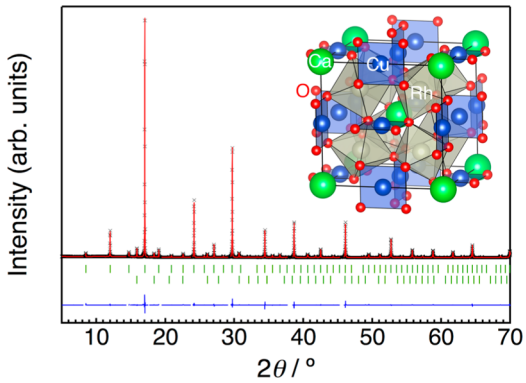

Figure 1. Observed SXRD pattern of CCRhO and the Rietveld refinement. Crosses (black) and solid lines (red) represent observed and calculated patterns, respectively. The difference between the observed and calculated patterns is shown at the bottom (blue). The vertical marks (green) indicate the Bragg reflection positions of CCRhO (upper) and RhO_2 (lower). The inset shows the drawing of the refined crystal structure of CCRhO.

of multiple constituent valence-variable TM ions. For most $CaCu_3B_4O_{12}$-type compounds, tetravalent TM ions primarily occupy the B sites, resulting in $Ca^{2+}Cu^{2+}{}_3B^{4+}{}_4O_{12}$ (B = Ti, V, Cr, Mn, Fe, Ru, Ir, Pt, Ge, Sn) valence states. In contrast, $CaCu_3Co_4O_{12}$ (CCCoO) contains Cu^{3+} ions in the $Ca^{2+}Cu^{3+}{}_3Co^{3.25+}{}_4O_{12}$ valence state.[6,7] Unusual high-valence states of late 3d TM ions (e.g., Fe^{4+}, Co^{4+}, and Cu^{3+}) are dominated by ligand holes in O 2p orbitals, as evidenced by negative charge-transfer energies.[7−10] The electron configurations of these TM ions are represented as $d^5\underline{L}^1$ (Fe^{4+}), $d^6\underline{L}^1$ (Co^{4+}), and $d^9\underline{L}^1$ (Cu^{3+}), where $\underline{L}$ represents a ligand hole. The

Received: June 8, 2014
Published: July 7, 2014

dx.doi.org/10.1021/ic501341x | *Inorg. Chem.* 2014, 53, 7089−7091

ligand holes are primarily ascribed to Cu ions for CCCoO and $YCu_3Co_4O_{12}$, and they are transferred between TM ions [$3Cu^{2+} + 4Fe^{3.75+}(d^5\underline{L}^{0.75}) \rightarrow 3Cu^{3+}(d^9\underline{L}^1) + 4Fe^{3+}$] or disproportionated [$2Fe^{4+}(d^5\underline{L}^1) \rightarrow Fe^{3+} + Fe^{5+}(d^5\underline{L}^2)$] in $ACu_3Fe_4O_{12}$ compounds (A = divalent alkaline-earth or trivalent rare-earth metal) with variations in the temperature.[11−13] These examples suggest that unusual high-valence TM ions facilitate various intriguing electronic states.

$CaCu_3Rh_4O_{12}$ (CCRhO) was recently investigated by first-principle calculations.[14] It was predicted that CCRhO consisted of unusual high-valence Cu^{3+} and normal-valence $Rh^{3.25+}$ ions rather than Cu^{2+} and Rh^{4+} ions. However, to our knowledge, a synthetic study of CCRhO was never reported. Here, we illustrate the high-pressure synthesis, crystal structure, and valence state of CCRhO. Synchrotron X-ray absorption (XAS) and photoemission spectroscopy revealed that CCRhO had a valence state of $Ca^{2+}Cu^{\sim 2.8+}{}_3Rh^{\sim 3.4+}{}_4O_{12}$, which was approximately consistent with the first-principle prediction.[14]

A polycrystalline sample of CCRhO was synthesized under a pressure and temperature of 15 GPa and 1273 K, respectively (see experimental and computational details in the Supporting Information, SI). Figure 1 shows the synchrotron X-ray powder diffraction (SXRD) pattern and the corresponding Rietveld refinement of CCRhO. The sample was nearly single-phase, except for small amounts of RhO_2 (∼5 wt %) and unknown impurities (presumably less than a few weight percent). The primary phase was indexed with a cubic $AA'_3B_4O_{12}$-type perovskite structure with a lattice constant, *a*, of ∼7.39 Å. Crystal structure refinement based on the SXRD data using the Rietveld program *RIETAN-FP*[15] yielded reliable structure parameters and metal−oxygen bond lengths with good reliability factors (see Table 1). The bond valence sum (BVS)[16] for Cu ions is heavily

Table 1. Refined Structural Parameters and Selected Bond Lengths for $CaCu_3Rh_4O_{12}$[a]

atom	site	U_{iso} (10^{-3} Å^2)	M−O (Å)
Ca	2*a*	8.1(9)	2.618(3) × 12
Cu	6*b*	2.37(18)	1.878(2) × 4
Rh	8*c*	2.11(7)	1.9931(9) × 6
O	24*g*	5.4(6)	

[a]Space group: $Im\bar{3}$ (No. 204); Å = 7.39267(5) Å. Atomic position: Ca 2*a* (0, 0, 0), Cu 6*b* (0, $^1/_2$, $^1/_2$), Rh 8*c* ($^1/_4$, $^1/_4$, $^1/_4$), O 24*g* (0.3109(3), 0.1695(3), 0). Reliability factors: R_{wp} = 5.111%, R_B = 1.344%, and goodness of fit (GOF) = 1.1150. The occupancy factors *g* for all atoms were fixed to 1.

dependent on the BVS parameter, l_0; the BVS value of +2.33 (l_0 = 1.649) implied divalency, +2.97 (l_0 = 1.739) trivalency, and +2.92, which was estimated from interpolation,[17] an intermediate valence close to trivalency. The BVS of Rh ions could not be determined from the Rh−O bond lengths because of the absence of reliable BVS parameters for Rh^{4+} ions.

Spectroscopic measurements were performed to estimate the valence states of the constituent TM ions in CCRhO. Figure 2a shows the Cu $L_{2,3}$-edge XAS data for CCRhO and a CuO reference. The L_3-edge XAS spectrum of CCRhO consisted of a main peak at ∼932 eV and a shoulder at ∼930.5 eV. The position of the main peak was close to those of Cu^{3+} oxides.[18,19] The shoulder peak position of the Cu L_3-edge of CCRhO was identical with that of CuO, which was attributed to a divalent state. This indicated that the Cu ions in CCRhO had a mixed-valence state such as $Cu^{(2+\delta)+}$ (δ = 0−1). Figure 2b shows the O

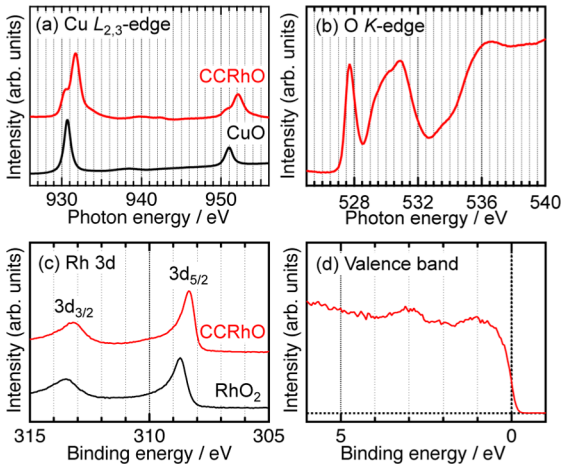

Figure 2. Soft XAS spectra of (a) Cu $L_{2,3}$-edge for CCRhO and CuO and (b) O K-edge for CCRhO. (c) HX-PES spectra of Rh 3d for CCRhO and RhO_2. (d) Valence band for CCRhO.

K-edge XAS spectrum of CCRhO. The O K-edge XAS spectrum consisted of mixed TM d and O 2p states. The structures at ∼530 and ∼535 eV were attributed to the Rh 4d and Cu 3d bands, respectively, which are commonly observed for $CaCu_3B_4O_{12}$ compounds.[20] In contrast, the intense peak at ∼527.5 eV confirmed that the Cu valence of CCRhO was higher than 2+.[21] Magnetic susceptibility data (see Figure S1 in the SI) exhibited a localized paramagnetic component [Curie constant *C* of 0.26(2) emu·K/mol] and a Pauli-like temperature-independent component [$\chi_0 = 2.32(6) \times 10^{-3}$ emu/mol]. In a simple approximation, the former is attributed to the Cu^{2+} spins ($S = {}^1/_2$), whereas the latter metallic conduction is governed by the Rh 4d electrons (the metallic character of CCRhO is shown later). In accordance with this approximation, it is estimated that ∼23% of the Cu ions existed in the Cu^{2+} state, although the rest of the Cu ions existed as low-spin $S = 0$ Cu^{3+} (see the energy diagram of 3d orbitals in the square-planar coordination in Figure S2 in the SI).[22] Therefore, the average valence of Cu ions was estimated to be ∼2.8.

The precise Cu valence was determined by calculations with the single impurity Anderson model considering the dynamical mean field.[23] Figure 3 shows the calculated Cu L_3-edge XAS

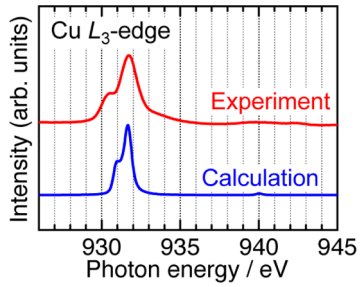

Figure 3. Calculated soft XAS spectrum of Cu L_3-edge for the $Cu^{2.8+}$ valence state. The experimental spectrum for CCRhO is also shown.

spectra in the $Cu^{2.8+}$ valence state. The spectral shape monotonically changed with varying valence states; the spectral weight was transferred from the lower-energy peak to the higher-energy peak with increasing valences, and eventually the two peaks merged into nearly a single peak at $Cu^{2.9+}$ (see Figure S3 in the SI). The experimental XAS spectrum was reasonably

dx.doi.org/10.1021/ic501341x | *Inorg. Chem.* 2014, 53, 7089−7091

described by the calculated spectrum for the $Cu^{2.8+}$ valence state, thus assuring that the Cu valence of CCRhO was approximately +2.8.

The Rh valence was investigated by hard X-ray photoemission spectroscopy (HX-PES). Figure 2c shows the Rh 3d core HX-PES spectrum of CCRhO, together with that of a RhO_2 reference. The binding energy of the Rh $3d_{5/2}$ main peak for CCRhO was 308.4 eV. This was shallower than that of RhO_2 by approximately 0.4 eV, indicating that the Rh ions of CCRhO were less oxidized than the Rh^{4+} ions of RhO_2. In accordance with charge neutrality, we conclude that the appropriate valence state of CCRhO is $Ca^{2+}Cu^{\sim 2.8+}{}_3Rh^{\sim 3.4+}{}_4O_{12}$. The Rh 4d electrons of CCRhO were expected to be in the low-spin configuration, because large crystal-field splitting is usually predominant in 4d electron systems in octahedral coordination, and Rh ions with a high-spin configuration have never been reported in rhodium oxides. Figure 2d shows the valence-band HX-PES spectrum of CCRhO. A significant spectral weight at the Fermi level indicated metallic character. This was consistent with the magnetization data in which a Pauli-paramagnetic-like component was substantial, as shown in Figure S1 in the SI.

CCRhO follows $CaCu_3Ru_4O_{12}$ (CCRuO) as the second member of $CaCu_3B_4O_{12}$-type compounds with B-site 4d TM ions. The paramagnetic metallic properties of CCRhO were similar to those of CCRuO.[24] However, the valence state of $Ca^{2+}Cu^{\sim 2.8+}{}_3Rh^{\sim 3.4+}{}_4O_{12}$ was different from that of CCRuO ($Ca^{2+}Cu^{\sim 2+}{}_3Ru^{\sim 4+}{}_4O_{12}$).[25] The origin of the high-valence Cu ions in CCRhO can be considered based on the relative energy levels of Cu 3d, Rh 4d, and O 2p orbitals, as suggested in ref 14. The Cu $d_{x^2-y^2}$ orbital lies at the highest energy level in the (pseudo-)square-planar coordination. Because of the large crystal-field splitting of the Rh 4d orbitals, the unoccupied Rh e_g orbitals occur at energy levels above the Fermi energy, while the Rh t_{2g} orbitals lie at energy levels slightly lower than or comparable to the Cu $d_{x^2-y^2}$ orbital in the vicinity of the Fermi energy. Thus, the partially occupied Cu $d_{x^2-y^2}$ and Rh t_{2g} orbitals result in intermediate valence states of $Cu^{2.8+}$ ($d^{8.2}$ or $d^9\underline{L}^{0.8}$) and $Rh^{3.4+}$ ($t_{2g}{}^{5.6}e_g{}^0$). This is different from other Cu^{3+}-containing $AA'_3B_4O_{12}$ perovskites, in which multiple late 3d TM ions compete for ligand holes. In $A^{3+}Cu_3Fe_4O_{12}$-type compounds, the Cu^{3+} valence state is achieved by the ligand hole transfer from Fe e_g–O 2p-hybridized orbitals to Cu $d_{x^2-y^2}$–O 2p orbitals with similar energy levels.[26] On the other hand, the large crystal-field splitting of Rh 4d orbitals preferentially generates unusual high-valence Cu ions in CCRhO, suggesting that the crystal-field splitting energy is a crucial factor in determining the valence states of complex TM oxides.

■ ASSOCIATED CONTENT

Supporting Information

Experimental details, energy level diagram of 3d orbitals in the square-planar coordination, magnetic susceptibility data, and crystallographic data of CCRhO in CIF format. This material is available free of charge via the Internet at http://pubs.acs.org.

■ AUTHOR INFORMATION

Corresponding Author

*E-mail: i-yamada@21c.osakafu-u.ac.jp.

Notes

The authors declare no competing financial interest.

■ ACKNOWLEDGMENTS

We thank Kengo Oka and Masaki Azuma for their assistance with XAS measurements. Synchrotron radiation experiments were performed at SPring-8 with the approval of the Japan Synchrotron Radiation Research Institute (Proposal Nos. 2011B1009, 2012B1171, 2013A1042, 2013A1689, 2013B1753, and 2014A1224). This work was carried out under the Visiting Researcher's Program of Geodynamics Research Center, Ehime University.

■ REFERENCES

(1) Imada, M.; Fujimori, A.; Tokura, Y. *Rev. Mod. Phys.* **1998**, *70*, 1039–1263.
(2) Momma, K.; Izumi, F. *J. Appl. Crystallogr.* **2011**, *44*, 1272–1276.
(3) Ramirez, A. P.; Subramanian, M. A.; Gardel, M.; Blumberg, G.; Li, D.; Vogt, T.; Shapiro, S. M. *Solid State Commun.* **2000**, *115*, 217–220.
(4) Alonso, J. A.; Sanchez-Benitez, J.; De Andres, A.; Martinez-Lope, M. J.; Casais, M. T.; Martinez, J. L. *Appl. Phys. Lett.* **2003**, *83*, 2623–2625.
(5) Yamada, I.; Tsuchida, K.; Ohgushi, K.; Hayashi, N.; Kim, J.; Tsuji, N.; Takahashi, R.; Matsushita, M.; Nishiyama, N.; Inoue, T.; Irifune, T.; Kato, K.; Takata, M.; Takano, M. *Angew. Chem., Int. Ed.* **2011**, *50*, 6579–6582.
(6) Yamada, I.; Ishiwata, S.; Terasaki, I.; Azuma, M.; Shimakawa, Y.; Takano, M. *Chem. Mater.* **2010**, *22*, 5328–5332.
(7) Mizokawa, T.; Morita, Y.; Sudayama, T.; Takubo, K.; Yamada, I.; Azuma, M.; Takano, M.; Shimakawa, Y. *Phys. Rev. B* **2009**, *80*, 124105.
(8) Mizokawa, T.; Fujimori, A.; Namatame, H.; Takeda, Y.; Takano, M. *Phys. Rev. B* **1998**, *57*, 9550–9556.
(9) Bocquet, A. E.; Fujimori, A.; Mizokawa, T.; Saitoh, T.; Namatame, H.; Suga, S.; Kimizuka, N.; Takeda, Y.; Takano, M. *Phys. Rev. B* **1992**, *45*, 1561–1570.
(10) Potze, R. H.; Sawatzky, G. A.; Abbate, M. *Phys. Rev. B* **1995**, *51*, 11501–11506.
(11) Yamada, I.; Takata, K.; Hayashi, N.; Shinohara, S.; Azuma, M.; Mori, S.; Muranaka, S.; Shimakawa, Y.; Takano, M. *Angew. Chem., Int. Ed.* **2008**, *47*, 7032–7035.
(12) Long, Y. W.; Hayashi, N.; Saito, T.; Azuma, M.; Muranaka, S.; Shimakawa, Y. *Nature* **2009**, *458*, 60–63.
(13) Yamada, I.; Etani, H.; Tsuchida, K.; Marukawa, S.; Hayashi, N.; Kawakami, T.; Mizumaki, M.; Ohgushi, K.; Kusano, Y.; Kim, J.; Tsuji, N.; Takahashi, R.; Nishiyama, N.; Inoue, T.; Irifune, T.; Takano, M. *Inorg. Chem.* **2013**, *52*, 13751–13761.
(14) Mukherjee, S.; Sarkar, S.; Saha-Dasgupta, T. *J. Mater. Sci.* **2012**, *47*, 7660–7664.
(15) Izumi, F.; Momma, K. *Solid State Phenom.* **2007**, *130*, 15–20.
(16) Brown, I. D.; Altermatt, D. *Acta Crystallogr., Sect. B: Struct. Sci.* **1985**, *41*, 244–247.
(17) Attfield, J. P. *Solid State Sci.* **2006**, *8*, 861–867.
(18) Mizokawa, T.; Konishi, T.; Fujimori, A.; Hiroi, Z.; Takano, M.; Takeda, Y. *J. Electron Spectrosc. Relat. Phenom.* **1998**, *92*, 97–101.
(19) Sarma, D. D.; Strebel, O.; Simmons, C. T.; Neukirch, U.; Kaindl, G.; Hoppe, R.; Muller, H. P. *Phys. Rev. B* **1988**, *37*, 9784–9787.
(20) Xin, Y.; Zhou, H. D.; Cheng, J. G.; Zhou, J. S.; Goodenough, J. B. *Ultramicroscopy* **2013**, *127*, 94–99.
(21) Vanveenendaal, M. A.; Sawatzky, G. A. *Phys. Rev. B* **1994**, *49*, 3473–3482.
(22) Chen, W.; Long, Y. W.; Saito, T.; Attfield, J. P.; Shimakawa, Y. *J. Mater. Chem.* **2010**, *20*, 7282–7286.
(23) Hariki, A.; Ichinozuka, Y.; Uozumi, T. *J. Phys. Soc. Jpn.* **2013**, *82*, 023709.
(24) Labeau, M.; Bouchu, B.; Joubert, J. C.; Chenavas, J. *J. Solid State Chem.* **1980**, *33*, 257–261.
(25) Hollmann, N.; Hu, Z.; Maignan, A.; Gunther, A.; Jang, L. Y.; Tanaka, A.; Lin, H. J.; Chen, C. T.; Thalmeier, P.; Tjeng, L. H. *Phys. Rev. B* **2013**, *87*, 155122.
(26) Rezaei, N.; Hansmann, P.; Bahramy, M. S.; Arita, R. *Phys. Rev. B* **2014**, *89*, 125125.